Efficient Single Photon Detection by Quantum Dot Resonant Tunneling Diodes

J. C. Blakesley,[1,2] P. See,[1] A. J. Shields,[1] B. E. Kardynał,[1] P. Atkinson,[2] I. Farrer,[2] and D. A. Ritchie[2]

[1]*Toshiba Research Europe Ltd., 260 Cambridge Science Park, Milton Road, Cambridge CB4 0WE, United Kingdom*

[2]*Cavendish Laboratory, University of Cambridge, Madingley Road, Cambridge CB3 0HE, United Kingdom*

(Received 10 June 2004; revised manuscript received 15 October 2004; published 16 February 2005)

We demonstrate that the resonant tunnel current through a double-barrier structure is sensitive to the capture of single photoexcited holes by an adjacent layer of quantum dots. This phenomenon could allow the detection of single photons with low dark count rates and high quantum efficiencies. The magnitude of the sensing current may be controlled via the thickness of the tunnel barriers. Larger currents give improved signal to noise and allow sub-μs photon time resolution.

DOI: 10.1103/PhysRevLett.94.067401 PACS numbers: 85.60.Gz, 85.30.–z, 85.35.Be, 85.35.Gv

Practical systems for optical quantum information technology require efficient, low noise single-photon detection. Often, however, the characteristics of single-photon detectors impose stringent limitations on the applicability of these techniques. For example, afterpulses due to trapped carriers restrict the maximum bit rate and reach of fiber-based quantum cryptography systems using avalanche photodiodes [1,2], while the limited detection efficiency and lack of a photon number resolving capability are barriers to linear optics quantum computing [3]. It is therefore desirable to explore novel detection methodologies. Photon detectors based on directly sensing a single photoexcited carrier would avoid avalanche multiplication and its associated problems. Single electron readout is also required for several solid-state quantum computing schemes [4–7]. We show here that single electrons or holes confined within a nanoscale quantum dot may be sensed via the effect of their electrostatic potential upon a resonant tunneling process. This allows efficient, low noise detection of single photons as well as a method of detecting single quantum charges.

The natural growth modes of strained epitaxial semiconductor layers provide an attractive method of forming quantum dots that can easily be incorporated into heterostructure devices [8]. Because of their nanoscale dimensions these ''self-assembled'' quantum dots behave like artificial atoms within the layer structure. By spectrally filtering the emission to collect just one transition, a quantum dot has been used to generate both optically and electrically excited single-photon pulses [9–11]. Quantum dots also make effective traps for electrons or holes [12]. Transistor structures containing a layer of quantum dots have been demonstrated as optically written floating gate memories [13,14] and midinfrared light detectors [15]. When etched to small areas, these transistor structures can be switched by individual photons [16]. However, the narrow channel layer in such transistors has limited their photon switching probability to $<1\%$.

We study the effect of single photocharges upon resonant tunneling processes using the structure shown schematically in Fig. 1(a). This consists of an n^+-i-n^+ semiconductor diode in which the intrinsic region contains a double-barrier tunnel structure and a layer of self-assembled quantum dots. The current flowing between the emitter and the collector contacts in response to an applied voltage is limited by tunneling through the double-barrier structure [17]. A sharp resonance in the tunnel current is observed for those voltages where the energy of electrons behind the emitter side barrier aligns with a confined level in the quantum well between the barriers [Fig. 1(c)]. Electrons trapped within the quantum dots induce a potential which affects the tunneling characteristics. As discussed later, neutralization of this trapped charge by photoexcited holes strongly affects the tunnel current of the diode, allowing the detection of individual photons.

The samples were grown by molecular beam epitaxy on a semi-insulating GaAs substrate. A typical layer structure

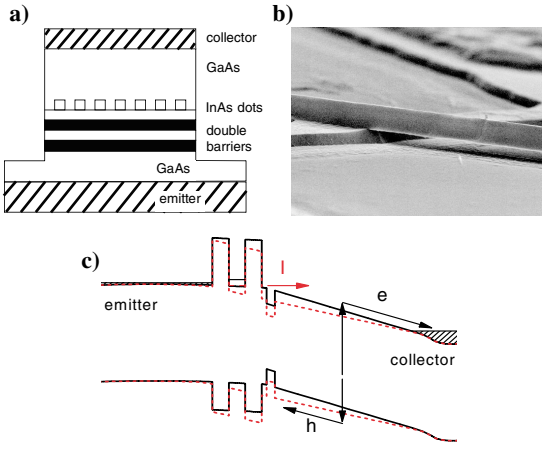

FIG. 1 (color). (a) Schematic of the device structure. (b) Scanning electron microscope image of a cross-wire structure with an active area of about 1 μm^2. The top wire forms a bridge between a contact pad (not shown) and the bottom wire, using an air gap for isolation. (c) Schematic band diagram of structure under forward bias, close to resonance. Capture of a single photoexcited hole by a quantum dot lowers the potential of the dot and alters the resonant tunneling condition (red dashed line).

consisted of a 200 nm GaAs buffer, a 10 nm AlAs etch-stop layer, a 230 nm GaAs emitter with graded n-type doping from 1×10^{18} to 1×10^{16} cm^{-3}, a 20 nm undoped GaAs spacer, a 10 nm $Al_{0.33}Ga_{0.67}As$ barrier, a 10 nm GaAs well, a 10 nm $Al_{0.33}Ga_{0.67}As$ barrier, a 2 nm GaAs spacer, an InAs self-assembled quantum dot layer, a 310 nm undoped GaAs intrinsic region, and a 50 nm n^+ doped GaAs collector. The layer of quantum dots was grown in the Stranski-Krastanov mode by depositing InAs on top of the GaAs [8]. The growth conditions for the quantum dot layer were designed to give a dot density of about 100 μm^{-2}. The thick intrinsic region above the quantum dots serves as a light absorbing layer.

Small tunnel junction area devices, shown in the scanning electron microscopy (SEM) image of Fig. 1(b), were fabricated in a cross-wire geometry [18]. This involved first etching a 1 μm wide top contact wire. Then a bottom contact wire was etched perpendicular to the top wire. A selective wet etch was used such that the top contact wire was undercut to form a freestanding bridge away from the junction where the two wires intersect. The only contact between the top and the bottom wires occurs where they cross, giving a contact area of about 1 μm square. Apart from its small active area, the cross-wire design is favorable because it avoids placing Ohmic contacts directly above the optically active area of the device. For comparison we also fabricated large-area structures by etching square mesas with sides of between 5 and 50 μm, using conventional techniques.

Figure 2(a) plots the current-voltage characteristic of a large-area sample with 10 nm $Al_{0.33}Ga_{0.67}As$ barriers measured at 4 K. A peak is seen in the characteristic for both forward and reverse biases corresponding to resonant tunneling through the double-barrier structure [19]. Notice that the resonance is much broader in forward bias. This is because the quantum dots in the intrinsic region trap electrons and induce an irregular potential across the surface of the double-barrier structure, which smears the tunneling resonance. In reverse bias, however, the degenerate electron gas which forms behind the collector-side barrier screens the potential of the dots. Under illumination the forward bias tunneling peak shifts to lower voltage [Fig. 2(b)]. The stronger the illumination, the more the peak bias shifts. We attribute this to the neutralization of charge in the quantum dots by photoholes generated in the thick intrinsic region.

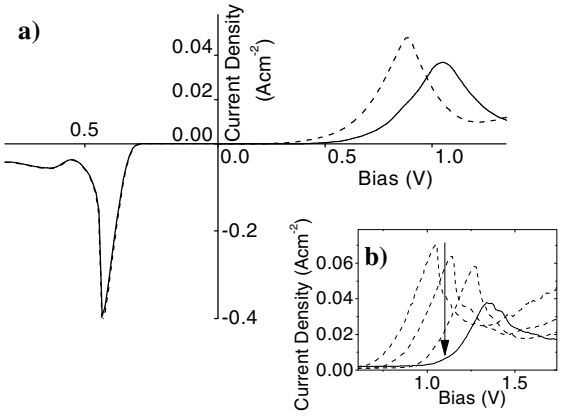

FIG. 2. (a) Current-voltage characteristic of a 10 $\mu m \times$ 10 μm mesa device with 10 nm $Al_{0.33}Ga_{0.67}As$ barriers at 4 K, measured with 100 nW cm^{-2} (dashed line) and without (solid line) illumination. Illumination causes the forward bias tunneling resonance to shift to lower bias due to the capture of photoexcited holes in the dots. (b) Forward bias tunnel resonance for illumination intensities from 1 to 100 nW cm^{-2} for a 1 μm^2 cross-wire device (arrow shows bias used for single-photon detection).

Time-resolved measurements were carried out on the samples at 5 and 77 K. A voltage was applied to bias them in the positive differential conductance region between the threshold and the peak bias [marked by the arrow in Fig. 2(b)]. The devices were illuminated continuously for a fixed period of time. The light source was then switched off for an equal period of time. This sequence was repeated for different intensities of light.

In the large-area samples, illumination caused a steady increase of tunnel current consistent with the shift of the tunnel peak in Fig. 2. After illumination the tunnel current returned to its initial value. The small-area structures showed the same behavior except that, instead of a continuous change, the tunnel current was observed to evolve with time in discrete, sharp steps [see Fig. 3(a) recorded at 5 K]. It can be seen that during illumination there are both positive and negative steps [(i) in Fig. 3(a)]. When the light source was switched off, the upwards steps ceased to occur and the tunnel current returned to its original value by a series of downwards steps [(ii) in Fig. 3(a)]. The discrete steps have also been observed clearly at 77 K.

We believe that these steps are due to the charging and discharging of individual quantum dots in response to the trapping of individual photoholes. When a photohole is captured by a dot, the negative charge on the dot is temporarily reduced until it is repopulated by the tunnel current. This results in a temporary reduction in the potential of the dot. The change in field brings the diode closer to resonance in the locality of the dot, causing a temporary rise in tunnel current. This is observed as a steplike increase in current through the structure, followed after a delay by a similar sized downwards step as the dot is repopulated. Since each photon absorbed produces just one hole, each upwards step corresponds to the absorption of a single photon.

Further evidence that the upward steps are single-photon induced is provided by the dependence on the incident photon flux. The rate of upward steps was measured by counting the number of times the differential (with respect to time) current crossed a threshold (discriminator) level. A calibrated, monochromatic light source was used so that the rate of photons hitting the active area of the device was known. Figure 3(b) shows the upward step rate for a discriminator level of 1 pA s^{-1} against the rate of incident

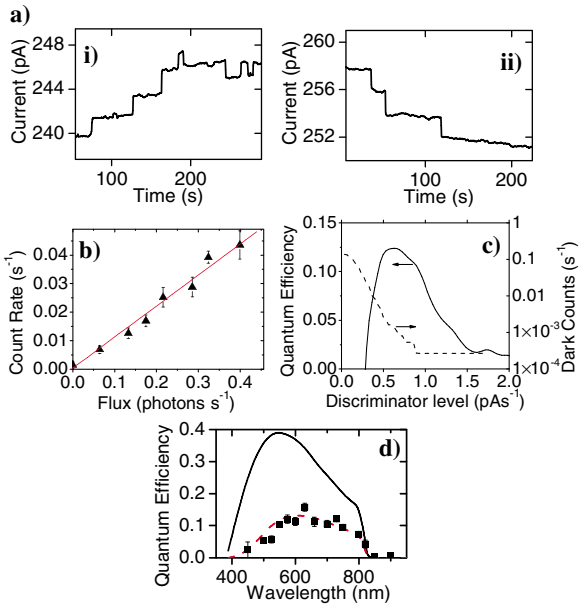

FIG. 3 (color). (a) Time-resolved measurements of a cross-wire device with 10 nm $Al_{0.33}Ga_{0.67}As$ barriers at 5 K: (i) under constant illumination with a red LED of about 0.2 photons per second per μm^2; (ii) after illumination has been switched off. (b) Rate of upwards steps counted with 1 pA s^{-1} discriminator level versus rate of incident photons from a 550 nm source on the active device area in a cross-wire device. Best fit (red line) giving a quantum efficiency of 10.9% for this particular discriminator level. (c) Quantum efficiency (solid line) and dark count rate (dotted line) versus step-counting discriminator level of a cross-wire device using 550 nm light. (d) Quantum efficiency as a function of wavelength of a cross-wire device with 310 nm intrinsic GaAs absorbing layer. Calculated fraction of incident light absorbed in intrinsic GaAs layer (solid curve) and calculated absorption within bottom 150 nm of intrinsic GaAs layer (red dashed curve).

photons at 550 nm for a cross-wire structure. The data show that the number of steps counted is linearly dependent on the number of incident photons, as expected for a single-photon process, with a quantum efficiency of $(10.9 \pm 1.5)\%$.

Figure 3(c) shows how the quantum efficiency and the dark count rate vary with the step-counter discriminator level for the same sample. From this, it can be seen that a maximum detection efficiency of 12.5% can be obtained by compromising on the dark count rate. For this discriminator level the dark count rate is about 2×10^{-3} s^{-1}. This can be reduced to values less than 3×10^{-4} s^{-1} while retaining detection efficiencies greater than 5%. The dominant contribution to the dark count rate derives from electrical noise from external sources and stray background light.

Figure 3(d) shows the quantum efficiency of a cross-wire structure as a function of the wavelength of incident light. The detection efficiency increases sharply for wavelengths shorter than 820 nm due to interband absorption into the thick GaAs layer containing the quantum dots. For wavelengths below 400 nm, the quantum efficiency reduces due to strong absorption of the incident light in the collector contact layer. Photoholes generated in the contact layer recombine without being captured by the dots. The solid line in Fig. 3(d) plots the calculated total absorption in the 310 nm intrinsic GaAs region. Notice that the measured detection efficiency is less than the total absorption in the intrinsic region and that the measured maximum efficiency lies to longer wavelength than the calculation. Both observations suggest that photoholes generated closer to the dots are more likely to be detected. Indeed, a much better fit is given by the red dashed curve, which assumes that only photons absorbed within 150 nm of the quantum dot layer are detected. This may be due to the surface charge at the sidewalls that tends to attract holes generated in the upper portion of the intrinsic region. Modifying the thickness of the intrinsic region and the contact region or passivating the surface leads to an increase in quantum efficiency. For example, if the thick intrinsic region is reduced to 150 nm, the collector contact is reduced to 20 nm, and an antireflection coating is applied, then we estimate a quantum efficiency of about 65% could be achieved.

The magnitude of the tunnel current may be controlled via the thickness of the barrier layers. Structures with 3 nm barriers have tunnel currents several orders of magnitude larger than those with 10 nm barriers. This has the effect of enhancing the strength of the single-photon signal. The larger signal can then be detected with a greater bandwidth and hence better time resolution while maintaining an acceptable signal-to-noise ratio. To achieve this, the tunnel current from 3 nm barrier devices was amplified using an amplifier with a low temperature first stage [20] and measured directly on a digital oscilloscope. Figure 4(a) plots a single trace of the tunnel current under weak illumination recorded at 4 K. The step in the tunnel current is induced by the capture of a single photoexcited hole by a dot, as discussed above, but now recorded over much faster time scales. In addition, as the barrier thickness was changed, the rate of repopulation of the dots (downwards steps) increased in proportion with the peak current, from a repopulation lifetime of the order 100 s in a 10 nm barrier sample to about 100 μs in a 3 nm barrier sample.

Using high-bandwidth differentiating electronics, each step can be converted into a pulse, as shown in the upper portion of Fig. 4(a). This allows the rate of photon induced pulses above a certain discriminator level to be counted using conventional pulse counting electronics. Figure 4(b) plots the count rate on a pulse counter with a 200 ns gate as a function of the discriminator level with the device under pulsed-laser illumination at 684 nm and in the dark. From this figure it can be seen that setting the discriminator level to be larger than about 30 mV allows the photon induced counts to be distinguished above counts due to noise. The flux used in this figure was approximately 0.15 photons per laser pulse, though this is subject to a systematic error due to uncertainties in optical alignment. The quantum efficiency for this sample is comparable to that of the 10 nm

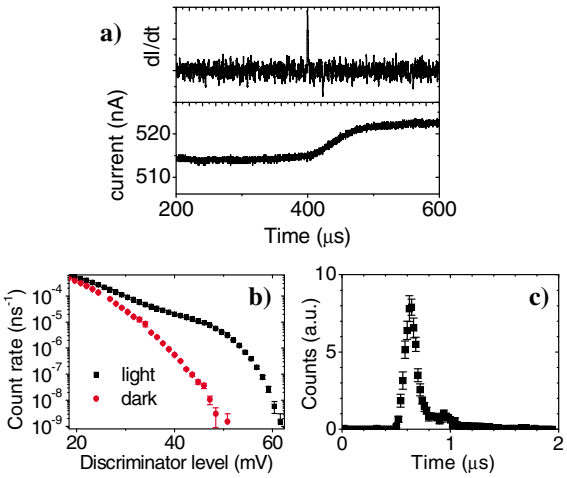

FIG. 4 (color). (a) Time-resolved measurements of a cross-wire device with 3 nm $Al_{0.33}Ga_{0.67}As$ barriers at 4 K. Lower portion: output of current amplifier showing a photon induced step (rise time is limited by the bandwidth of the dc amplifier). Upper portion: output of high-bandwidth differentiating electronics. (b) Count rate of photon induced pulses under illumination and in the dark as a function of discriminator level using a pulse-counter gate time of 200 ns. (c) Temporal response of the device in response to <1 photon laser pulses.

barrier sample. Setting the discriminator to 35 mV yields a quantum efficiency of about 5% with a dark count rate of 4×10^{-6} ns^{-1}, while a 45 mV discriminator gives a dark count rate of 5×10^{-8} ns^{-1} with an efficiency of approximately 1%.

The transient response of the detector was recorded by illuminating with a periodic train of laser pulses with a wavelength of 684 nm, a repetition rate of 250 kHz, and an average number of photons per pulse much less than one after beam attenuation. Figure 4(c) plots the count rate with a 50 ns gate time, recorded as a function of the gate delay after each laser pulse. The peak demonstrates a jitter in the photon detection time of about 150 ns, in principal allowing resolution of single-photon pulses generated at a rate of more than 5 MHz. The jitter originates from the rise time of the single-photon pulse, which is limited by the large capacitance of the external connections to the sample. A faster response could be achieved by using device packaging and leads optimized for high frequency operation. The maximum sustainable detection rate is limited by the rate at which the quantum dots can repopulate. Since there are approximately 100 quantum dots in the active region of a cross-wire device, the maximum count rate would be about 1 MHz for 3 nm barrier devices. Above this, we would expect to see a saturation of the quantum efficiency, though we have been unable to test this limit with our current experimental setup. We predict that the optimum barrier thickness for high-speed operation would be about 1 nm. Below this, the resonant tunneling peak will broaden significantly. If the observed trends continue, we would expect such a 1 nm barrier device to have a maximum sustainable detection rate of 10–100 MHz and jitter of less than 1 ns with an optimized amplifier. For even faster rates, the use of different resonant structures or the engineering of quantum dots for faster repopulation times should be investigated.

In conclusion, we have demonstrated that it is possible to detect the capture or the loss of a single charge in a quantum dot by sensing a change in the resonant tunneling current through a double-barrier structure. This phenomenon has been used for low noise detection of single photons with an efficiency of up to 12.5% and time resolution of 150 ns. This phenomenon is most suitable for applications requiring low noise detection of weak photon fluxes with modest timing resolution. An example of such an application is quantum cryptography, where count rates are typically 10^{-3} to 10^{-5} per clock cycle due to channel attenuation and where timing resolution to within one clock cycle is sufficient. With further optimization this effect could be useful for more general photon detection applications, as well as single electron detection in various quantum computing schemes.

[1] N. Gisin *et al.*, Rev. Mod. Phys. **74**, 145 (2002).
[2] C. Gobby, Z. L. Yuan, and A. J. Shields, Appl. Phys. Lett. **84**, 3762 (2004).
[3] E. Knill, R. Laflamme, and G. J. Milburn, Nature (London) **409**, 46 (2001).
[4] A. Imamoglu *et al.*, Phys. Rev. Lett. **83**, 4204 (1999).
[5] B. E. Kane, Nature (London) **393**, 133 (1998).
[6] M. H. Devoret and R. J. Schoelkopf, Nature (London) **406**, 1039 (2000).
[7] J. M. Elzerman *et al.*, Nature (London) **430**, 431 (2004).
[8] D. Bimberg, M. Grundmann, and N. N. Ledentsov, *Quantum Dot Heterostructures* (Wiley, New York, 1999).
[9] P. Michler *et al.*, Science **290**, 2282 (2000).
[10] Z. L. Yuan *et al.*, Science **295**, 102 (2002).
[11] C. Santori *et al.*, Phys. Rev. Lett. **86**, 1502 (2001).
[12] T. Lundstrom *et al.*, Science **286**, 2312 (1999).
[13] G. Yusa and H. Sakaki, Appl. Phys. Lett. **70**, 345 (1997).
[14] J. J. Finley *et al.*, Appl. Phys. Lett. **73**, 2618 (1998).
[15] S.-W. Lee, H. Hirakawa, and Y. Shimada, Appl. Phys. Lett. **75**, 1428 (1999).
[16] A. J. Shields *et al.*, Appl. Phys. Lett. **76**, 3673 (2000).
[17] H. Mizuta and T. Tanoue, *The Physics and Applications of Resonant Tunnelling Diodes* (Cambridge University Press, Cambridge, 1995).
[18] J. Wang *et al.*, Appl. Phys. Lett. **65**, 1124 (1994).
[19] We define forward bias as a positive voltage applied to the collector with respect to the emitter. This has the effect of lowering the collector potential with respect to the emitter, as shown in Fig. 1(c).
[20] B. E. Kardynal *et al.*, Appl. Phys. Lett. **84**, 419 (2004).